

# EXPERIMENTAL OPTIMIZATION OF THE PERFORMANCE AND RELIABILITY OF STAND-ALONE PHOTOVOLTAIC SYSTEMS

David L. King, Thomas D. Hund, William E. Boyson, and Jay A. Kratochvil  
Sandia National Laboratories, Albuquerque, NM, 87185-0752

## ABSTRACT

Stand-alone photovoltaic systems are deceptively complex. Optimizing the performance and reliability of these systems requires a complete understanding of their behavior as a function of site-dependent environmental conditions. Individual component specifications provide useful design information. However, to fully understand the interactions between components, it is necessary to simultaneously characterize the performance of the system and its separate components under actual operating conditions. This paper describes how a new 30-day outdoor testing procedure was coupled with array performance modeling to accomplish this objective. The procedure measures battery capacity, determines appropriate set-points for charging, and based on daily intervals quantifies dc-energy available from the array, charge-controller efficiency, battery efficiency, inverter efficiency, overall system efficiency, days of autonomy, and ac-energy available by month.

## INTRODUCTION

In collaboration with system integrators, Sandia conducts comprehensive evaluation and experimental optimization of stand-alone and hybrid photovoltaic systems with the primary objective of identifying areas for improvement in performance, reliability, and safety. These evaluations are conducted at the request of the system integrator and address performance of individual components, system functionality, safety concerns, and compliance with applicable codes and standards. Figures 1 and 2 are photos of typical systems evaluated. The procedure developed and the insight gained from this work will benefit the effort to develop standardized test procedures for stand-alone systems [1].

## ARRAY PERFORMANCE CHARACTERIZATION

The module and array performance characterization procedures used at Sandia have been documented elsewhere [2, 3, 4]. The combination of testing and modeling provides the following information: (1) electrical performance of the array at the ASTM Standard Reporting Condition [5]; (2) calculated annual and monthly dc-energy available from the array [6]; (3) temperature coefficients for  $I_{sc}$ ,  $I_{mp}$ ,  $V_{oc}$ ,  $V_{mp}$ , and  $P_{mp}$ ; (4) solar spectral (absolute air mass,  $AM_a$ ) influence on  $I_{sc}$  for clear sky conditions; (5) solar angle-of-incidence influence on  $I_{sc}$  for clear sky

conditions; (6) performance model with coefficients appropriate for all operating conditions; and (7) a relationship for array operating temperature versus solar irradiance, ambient temperature, and wind speed.



Fig. 1: 640-W<sub>p</sub> stand-alone system with 24-Vdc, 700-Ah battery bank, and 2.4-kW inverter.



Fig. 2: 600-W<sub>p</sub> stand-alone system with 24-Vdc, 440-Ah battery bank, and 2.4-kW inverter.

The electrical, thermal, and optical performance characteristics determined were used in our performance model to calculate the maximum dc-energy available from the photovoltaic array on a daily basis for the entire year for different sites. For instance, assuming the array can be oriented at different tilt-angles and is facing south, the performance model used hourly-average solar resource and meteorological data for Albuquerque to calculate daily-

average dc-energy production by month. The hourly solar resource and weather data used were “typical meteorological year” data from the National Solar Radiation Database [7]. Figure 3 shows the calculated dc-energy available from a 600-W<sub>p</sub> array at a latitude tilt-angle (35 degrees) and three other tilt orientations; 50, 60, and 20 degrees. The values given assumed that the array operated at its maximum-power-voltage ( $V_{mp}$ ) throughout the day. Therefore, these energy values provide an upper limit for the dc-energy available from the stand-alone photovoltaic system. In this case, tilt adjustment was definitely advantageous, particularly for worst-case winter conditions when the solar resource was lowest. A two-orientation strategy with tilt adjustment in mid-September and again in mid-March provided about 10% more dc-energy in winter and 5% more in summer relative to a single latitude-tilt orientation.

How well the dc-energy available from the array is utilized by the system depends strongly on the remaining components in the system (charge controller, battery, inverter, wiring). For instance, Figure 4 illustrates a typical situation where the distribution of array  $V_{mp}$  over the year is well above the system operating voltage dictated by the state-of-charge of the battery. In general, the upper edge of the scatter band of  $V_{mp}$  values occurs in the winter months, and the lower edge in summer. Without a maximum-power-point-tracking (MPPT) capability in the charge controller, there was an annual loss in Albuquerque of 15 to 20% of the dc-energy available from the array. This dc-energy loss will be greater in colder climates (Alamosa, CO) and less in hotter climates (Phoenix, AZ). Quantifying the energy flow into and out of all components is essential to understanding and optimizing overall system performance.

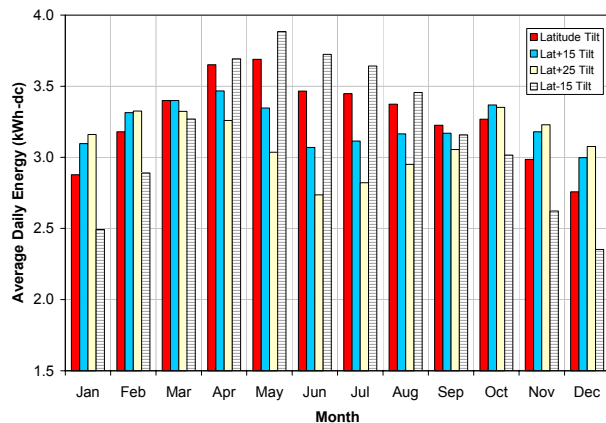


Fig. 3: Calculated daily dc-energy available from 600-W<sub>p</sub> array at different tilt orientations in Albuquerque, NM.

Figure 5 shows a schematic for a typical stand-alone system indicating energy flow and energy losses associated with each component. The locations for measurements required to quantify energy flow through components are also shown in the figure. Continuous data acquisition over an extended test period provides the information required to optimize system performance.

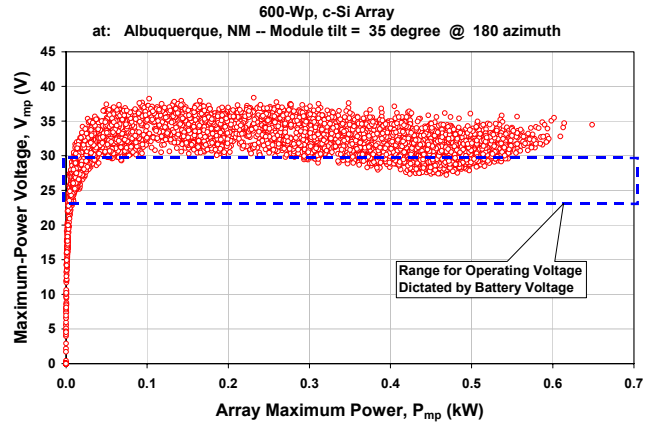


Fig. 4: Calculated hourly values for array maximum-power-voltage,  $V_{mp}$ , versus array maximum power,  $P_{mp}$ , for the entire year in Albuquerque.

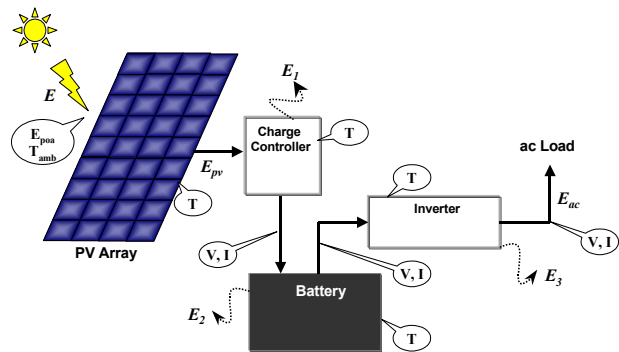


Fig. 5: Schematic of a typical stand-alone system showing energy flow and losses, along with measurements needed for characterizing system performance.

### 30-DAY SYSTEM TESTING PROCEDURE

A 30-day test procedure was developed to evaluate the functionality and safety of all system components and to test the performance of the system during ‘normal’ as well as ‘worst case’ operating conditions, without exceeding system design parameters. The ‘worst case’ condition discharged the batteries to the low-voltage-disconnect ( $V_{LVD}$ ) setpoint, and then required the system to recover to a full state-of-charge (SOC) while still powering the design load. The key to successful execution of the procedure was selecting a conservative (slightly undersized) ac-load and then scaling this daily ac-load in proportion to the previous day’s solar resource. This approach compensated for the unavoidable day-to-day variation in the solar insolation during the test period.

The system test procedure consisted of the following sequential steps: (1) installation and inspection of system, (2) calculation of appropriate ac-load to use during test sequence, (3) an initial battery test to verify manufacturer’s capacity specification and identify appropriate charge control setpoints, (4) multiple days of “cycling” during normal operation, (5) intentional battery discharge to the

system low-voltage-disconnect ( $V_{LVD}$ ) providing a measurement of 'usable' battery capacity, (6) multiple-day 'recovery test' from  $V_{LVD}$  including additional cycling after full state-of-charge was reached, (7) a second discharge to  $V_{LVD}$  to retest 'usable' battery capacity, and (8) a second 'recovery test' from  $V_{LVD}$  without an ac-load applied.

Figure 6 illustrates the last five steps of the test procedure in terms of the measured battery voltage and net capacity. Electrolyte specific gravity (SG) is also indicated at three points during the test sequence. System performance characteristics, setpoint verification, and energy losses associated with all system components were determined during actual operating conditions. For instance, the battery capacity was measured twice during the test sequence, providing data as illustrated in Figure 7. In the case illustrated, the 'usable' battery capacity, when discharged to the manufacturer recommended  $V_{LVD}=22.8$  V, was about 85% of rated capacity. For this system, the usable battery capacity provided about 4 days-of-autonomy without energy available from the PV array. Analysis also indicated that for flooded lead-acid batteries the  $V_{LVD}$  setting controlled by the Trace DR2424 inverter was too low and not adjustable, a situation likely to limit battery lifetime (reliability) if the ac-load frequently discharges the battery to the  $V_{LVD}$  condition. In addition, the low-voltage-reconnect setting,  $V_{LVR}$ , controlled by the DR2424 was also too low and not adjustable, resulting in unstable system operation due to insufficient recharging from a  $V_{LVD}$  condition before the ac-load was reconnected.

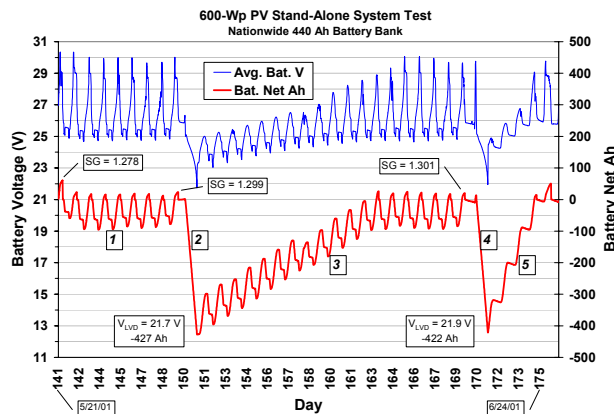


Fig. 6: Battery voltage and net capacity during five phases of system test procedure: cycling, capacity test, recovery and cycling, capacity test, recovery.

By using daily energy measurements, 'daily energy efficiency' was determined for the array, charge controller (MPPT efficiency), battery, inverter, and the overall system. In addition, a daily energy budget was determined that clearly illustrated the components most responsible for limiting overall system performance. Figure 8 illustrates an example of a stand-alone system with only 54% of the dc-energy available from the photovoltaic array provided to the ac-load. In this case, different component selection, charge-control setpoints, and operating strategy could increase the ac-energy available from the system by about 50%, and improve the overall system energy efficiency to about 75%. The dc-energy available from the array can be

increased using array tilt-angle adjustments, and by ensuring actual module performance meets the nameplate rating. Energy provided to the battery can be significantly increased by better matching array voltage characteristics to the battery operating voltage window or by using a charge controller with MPPT capability. Energy lost in the battery can be significantly reduced by careful attention to charge-controller setpoints and to the energy budgeted for periodic overcharging (equalization) necessary to maintain battery health. Finally, selection of an inverter with high efficiency and low dc tare loss is critical for achieving high overall system efficiency.

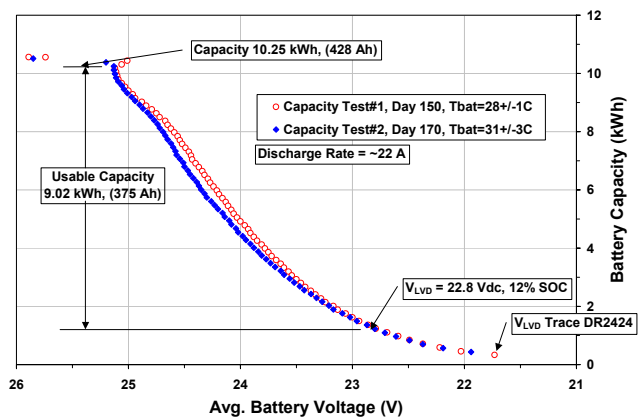


Fig. 7: Battery capacity (full and usable) versus battery voltage measured during 30-day test procedure.

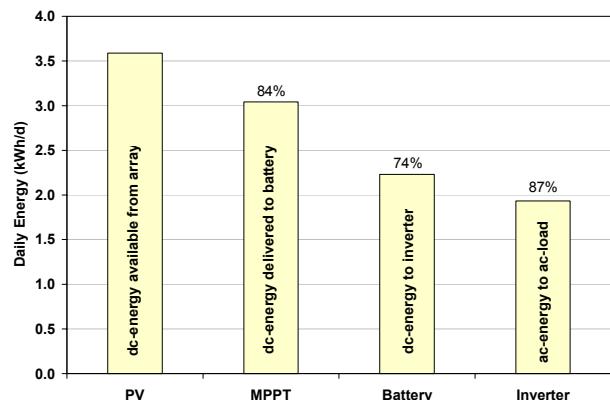


Fig. 8: Daily energy budget for 600-W<sub>p</sub> stand-alone PV system operating in Albuquerque in June, showing decrements in daily energy from array to ac-load, and daily energy efficiency for each component.

### MODEL FOR DAILY ENERGY EFFICIENCY

Analyzing energy flow on a daily basis provides an ideal method for simplifying stand-alone system test results, and for putting them in terms that are readily understandable for both the system designer and owner. The solar insolation on the array, energy available from the photovoltaic array, energy flow into and out of system components, as well as the ac-energy delivered by the system can all be expressed in units of kWh/d. This approach makes it possible to assign a 'daily efficiency' to

each major component in the system in terms of the ratio of daily energy out of the component divided by the daily energy into the component. In addition, a daily efficiency can be determined for the overall system as the ratio of the daily ac-energy provided by the system divided by the daily dc-energy available from the photovoltaic array. To be consistent with the format of commonly available solar resource data [6], and to take into account seasonal influences on system performance, the approach can also be expressed in terms of average daily efficiency for each month of the year. This modeling approach is expressed in Equations 1 and 2.

$$E_{ac} = (E_{SUN} \cdot A \cdot \eta_{PV}) \cdot \eta_{MPPT} \cdot \eta_{BAT} \cdot \eta_{INV} \quad (1)$$

or

$$E_{ac} = E_{PV} \cdot \eta_{MPPT} \cdot \eta_{BAT} \cdot \eta_{INV}$$

and

$$\eta_{SYS} = E_{ac} / E_{PV} \quad (2)$$

Where:

$E_{ac}$  = ac-energy delivered to the load by the system per day, (kWh/d, ac).

$E_{PV}$  = daily dc-energy available from the photovoltaic array at its maximum-power-point, (kWh/d, dc).

$E_{SUN}$  = solar energy available per day per square meter of module area, (kWh/m<sup>2</sup>d).

$A$  = sum of the areas of all modules in the array, (m<sup>2</sup>).

$\eta_{PV}$  = daily energy efficiency for the photovoltaic array calculated as the ratio of daily dc-energy available from the array, at its maximum-power-point, divided by the daily solar energy incident on the array.

$\eta_{MPPT}$  = daily energy efficiency for the charge controller, the ratio of the daily dc-energy out of the charge controller divided by the daily dc-energy available from the array. (MPPT efficiency)

$\eta_{BAT}$  = daily energy efficiency for the battery, the ratio of the daily dc-energy out of the battery divided by the daily dc-energy delivered by the charge controller.

$\eta_{INV}$  = daily energy efficiency for the inverter, the ratio of the daily ac-energy from the inverter divided by the daily dc-energy provided to the inverter.

$\eta_{SYS}$  = overall daily energy efficiency of the system, the ratio of the daily ac-energy to the load divided by the daily dc-energy available from the array.

It is important to recognize that the successful application of this testing and analysis procedure required the system to operate continuously for an extended period of time, without exceeding design limits. Otherwise, the daily energy efficiency concept can provide meaningless or unrealistic results. For instance, if the array provided no energy for an entire day, then the daily charge-controller efficiency ( $\eta_{MPPT}$ ) becomes zero. Similarly, if no energy was provided from the charge-controller during the day, but energy was still extracted from the battery, then its energy efficiency ( $\eta_{BAT}$ ) becomes meaningless.

## SYSTEM DESIGN AND SIZING

The system engineering insight gained from the testing and analysis approach summarized in this paper can improve and simplify the design procedure for stand-alone photovoltaic systems. Engineering analyses that

quantify the factors in Equation 1 can provide an adequate system design that is tailored to the site and application selected.

## CONCLUSIONS

Significant progress has been made in developing improved testing and modeling procedures needed to optimize stand-alone photovoltaic systems. Initial results from several systems have identified several opportunities for improvement in performance, reliability, safety, and mechanical design. Although not discussed in this paper, it is important that the enclosures used to house the battery and the inverter are designed to control operating temperature extremes, and to ensure that hydrogen gas generated during battery charging is adequately vented. Additional work is needed to better characterize inverter, charge controller, and battery performance as a function of operating temperature and age.

## ACKNOWLEDGEMENTS

The authors would like to acknowledge valuable discussions with the following: Ron Orozco (Energia Total), Steve Allen (Kyocera Solar), David Melton (Sacred Power), and Moneer Azzam (Solar Dynamics). *[Sandia is a multi-program laboratory operated by Sandia Corporation, a Lockheed Martin Company, for the United States Department of Energy under Contract DE-ACO4-94AL85000.]*

## REFERENCES

- [1] IEEE P1526/D3, "Draft Recommended Practice for Testing the Performance of Stand-Alone Photovoltaic Systems", June 2001.
- [2] D. King, et al., "Field Experience with a New Performance Characterization Procedure for Photovoltaic Arrays," *2<sup>nd</sup> World PVSEC*, 1998, pp. 1947-1952.
- [3] C. Whitaker, et al., "Application and Validation of a New PV Performance Characterization Method," *26<sup>th</sup> IEEE PVSC*, 1997, pp. 1253-1256.
- [4] B. Kroposki, et al., "Comparison of Module Performance Characterization Methods," *28<sup>th</sup> IEEE PVSC*, 2000, pp. 1407-1411.
- [5] ASTM E 1036, "Testing Electrical Performance of Non-concentrator Photovoltaic Modules and Arrays Using Reference Cells."
- [6] D. King, et al., "Analysis of Factors Influencing the Annual Energy Production of Photovoltaic Systems," *29<sup>th</sup> IEEE PVSC*, 2002, New Orleans.
- [7] Anon., "NSRDB Vol.2, National Solar Radiation Data Base, 1961-1990," NREL/TP-463-5784, 1995.